Steady and Unsteady Flow in a Side Heated Free Convection Loop Placed in Magnetic Field

Ahmed Jameel Kadhim and Ahmed M. Abdulhadi
Department of Mathematics, College Science, Baghdad University.
E-mail: Ahmed_Jameel8@ yahoo.com.

Abstract

In this study consideration is given to the hydrodynamic characteristics of a buoyancy-driven convection loop containing an electrically-conducting fluid in a transverse magnetic field in one-dimensional model. We study three problems. In problem one, we analyze the unsteady flow in closed loop in which the right side is isothermal heated and the left side is isothermal cooled, while the top and bottom regions are insulated. In problems two and three, we analyze the steady and unsteady flow in closed loop in which the bottom region is isothermal heated and the top region is isothermal cooled, while the right and left sides are insulated regions.

The Laplace transformation technique is used to solve problems one and three, while in problem two we found an analytical solution.

Keywords: Fluid Mechanic, Heat Transfer, Magnetofluiddynamics, Convection.

1. Introduction

Magnetofluiddynamics (MFD), [1], is that branch of applied mathematics which deal with the flow of electrically conducting fluids in electric and magnetic fields. It unifies in a common framework the electromagnetic and fluid-dynamic theories to yield a description of the concurrent effects of the magnetic field on the flow and the flow on the magnetic field.

There are many natural phenomena and engineering problems susceptible to magnetofluiddynamic (MFD) analysis. It is useful in astrophysics because much of the universe is filled with widely spaced, charged particles and permeated by magnetic fields, and so the continuum assumption becomes applicable. Again geophysicists encounter MFD phenomena in the interactions of conducting fluids,[3], and magnetic fields that are present in and around heavenly bodies. Engineers employ MFD principles in the design of heat exchangers, pumps, and flow meters; in solving space vehicle propulsion, control, and reentry problems; in designing communications and radar system; in creating novel power generating system; and in developing confinement schemes for controlled fusion.

Laminar natural convection flow in closed loops has been studied by many investigators since it has considerable number of practical applications in the design of thermal energy systems including thermosyphonic solar applications and nuclear technologies. When a transverse magnetic field is applied to an electrically conducting fluid in the loop, convective hydrodynamic motion is damped and an electric current is induced. Such a system has two principal applications: the first is in energy systems or industrial processes that require control of flow destabilization or prohibition of motion: the second interest lies in the possible use of the system for electricity generation.

In (1983) Hart [4] studied two-dimensional convection in a horizontal cavity, driven by differential heating of the two vertical end walls. In his paper, he describes the development of the unicellular flow and secondary instability of the unicell for shallow cavities filled with a low Prandtl number liquid. He shows that for prandtl numbers less than about 0.1, and aspect ratios less than the same value, parallel flow core will exist with approximately unit non-dimensional amplitude (a=1) up to the point ($Gr\sim800$) where secondary vortices appear.

In (1986) Vives [7] studied the role of natural and damped during the thermally controlled solidification of tin and aluminum alloys in a toroidal mould. The damped convection was caused by a stationary and uniform magnetic field parallel to the gravity field. In his paper, Vives shows that the

evolution of the thermal phenomena with time (or with the position of the solidification front) and also their interactions on the crystal growth were examined, for various degrees of superheat, both in the absence and presence of an axial and a stationary magnetic field.

N. Ghaddar in (1998) [2], studied the hydrodynamic characteristics of a buoyancy-driven convection loop containing an electrically-conducting fluid in a transverse magnetic field analytically using a one-dimensional model. One side of the loop is isothermally heated and the other side isothermally cooled, and the upper and lower sections are insulated. In her paper, the value of Prandtl number was taken from 0.003 to 7 and the value of Reynolds number was taken from 10 to150. She concluded that the closed-form solution of the flow velocity is used to predict the induced electric current of the system. And she found according to the solution there exist an optimal strength of the magnetic field that depends on the system flow and geometric parameters to maximize the induced electric current.

In this paper we will consider three problems, the first one is the unsteady state of Ghaddar's problem [2], the second and third are the steady and unsteady state respectively with the same loop as Fig. (1) with exception that the bottom part of the loop wall is isothermally heated to T_H, the top part isothermally cooled to T_C and the right and left side are insulated.

2. Problems Statement

A consideration is given to a loop 2L in height, an internal channel half width d. The upper and lower connecting portions of the vertical channel are semi-circular each of height l, see Fig.(1). The Boussinesg fluid contained in the loop is electrically conducting with an electrical conductivity σ, and a coefficient of thermal expansion β. The magnetic field B_0 is applied perpendicular to gravity in the x-direction. The thermophysical properties of the fluid at a fixed temperature T_0 are assumed to be constant except for the mass density ρ which is related to temperature according to

$$\rho = \rho_0\big(1 - \beta(T - T_0)\big) \quad \text{.....(1)}$$

Assuming the channel width of the loop to be much smaller than its length 2L, i.e., $2d < 2L$.

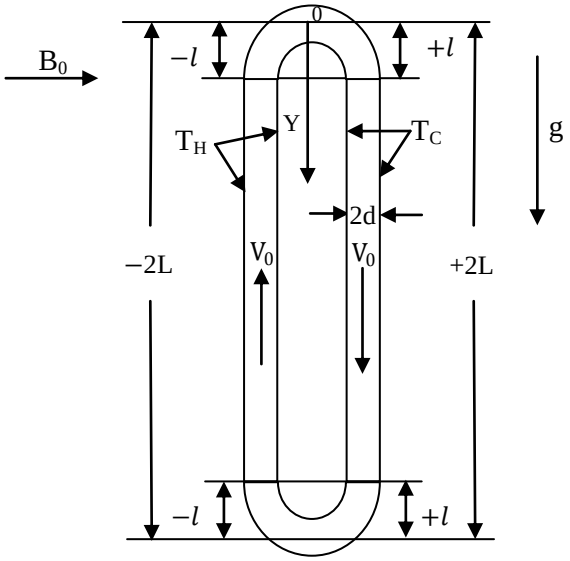

Fig.(1) The essential features of the thermosyphonic side-heated closed loop.

In all three problems, T_C , was taken as the reference temperature, and we will write down the energy equation in term of the bulk temperature , T_b , with this consideration equation (1) may be written as $\rho = \rho_0\big(1 - \beta(T_b - T_C)\big)$.

To simplify the coordinate system, circular ends at the top and bottom parts of the loop are considered to be straight and the origin of the y-axis placed at the top of the loop, parallel to the flow direction as it moves down with gravity along the cold side from 0 to +2L, and against gravity along the hot side from -2L to 0, with motion being clockwise.

3. Problem One

In this problem, we study the unsteady state of Ghaddar's problem [2], he study the steady state. Here, the left side of the loop wall is isothermally heated to T_H and the right side isothermally cooled to T_C.

3.1 The Continuity and Energy Equations

The continuity and the energy equations will be written in terms of bulk temperature. Also, to simplify the problem, the following assumptions are made.

1-The fluid velocity through the channel is constant and denoted by V_0.

2-The fluid is incompressible i.e. ρ=constant.

Using the assumptions mentioned above the continuity and energy equations for the problem under consideration can be written as

$V_0 = \text{constant}$ .....(2)

The energy equation for $-2L+l \le y \le -l$ and $l \le y \le 2L - l$

$$\rho C_p \left[\frac{\partial T_b}{\partial t} + V_0 \frac{\partial T_b}{\partial y}\right] = \frac{h}{2d}\{T_w - T_b\} + \sigma {V_0}^2 {B_0}^2 \quad \text{..... (3)}$$

And for the regions $-l \le y \le l$ and $2L - l \le y \ge -2L + l$

$$\rho C_p \left[V_0 \frac{\partial T_b}{\partial y}\right] = \sigma {V_0}^2 {B_0}^2 \quad \text{.....(4)}$$

Where T_b is the bulk temperature, T_w is the loop wall temperature in the isothermal regions defined by:

$T_w = T_H$ for $-2L + l \le y \le -l$ ..... (5 a)

$T_w = T_C$ for $l \le y \le 2L - l$ ..... (5 b)

By introducing the following new quantities:

$$\theta_b = \frac{T_b - T_C}{T_H - T_C},\ y^* = \frac{y}{d},\ t^* = \frac{tV_0}{d}$$

The dimensionless form of equations (3) and (4) can be written as:

$$\frac{\partial \theta_b}{\partial t^*} + \frac{\partial \theta_b}{\partial y^*} + m\theta_b = m + \frac{Ha^2 Ec}{Re} \quad \text{.....(6)}$$

for $-2L + l \le y \le -l$ and for $+l \le y \le 2L - l$

$$\frac{\partial \theta_b}{\partial t^*} + \frac{\partial \theta_b}{\partial y^*} + m\theta_b = \frac{Ha^2 Ec}{Re} \quad \text{.....(7)}$$

And the dimensionless form of the energy equations in the insulated region are

$$\frac{\partial \theta_b}{\partial y^*} = \frac{Ha^2 Ec}{Re} \quad \text{.....(8)}$$

for $-l \le y \le l$ and for $2L - l \le y \ge -2L + l$

$$\frac{\partial \theta_b}{\partial y^*} = \frac{Ha^2 Ec}{Re} \quad \text{.....(9)}$$

From which, by using the continuity condition, the boundary conditions that associated with the energy equations for the top and bottom regions are

$$\theta_b(l) = \theta_b(-l) + 2Ha^2 Ec(\tfrac{l}{d})/Re \quad \text{..... (10)}$$

$$\theta_b(-2L + l) = \theta_b(2L - l) + Ha^2 Ec(\tfrac{l}{d})/Re \quad \text{.....(11)}$$

And the initial condition is given by

$$\theta_b(y^*, t^*) = 0 \text{ at } t^* = 0 \quad \text{.....(12)}$$

Where m = $\frac{Nu}{2prRe}$ = Stanton number, Re = $\frac{v_0 d\rho}{\mu}$ =Reynolds number, $Ha = Bd\sqrt{\frac{\sigma}{\rho\nu}}$ = Hartmann number and $Ec = \frac{{v_0}^2}{C_p \triangle T}$ = Eckert number.

3.2 Method of Solution

The Laplace transformation technique,[6], is used to solve each of equations (6) and (7) and there analytic solution ,respectively, are

$$\theta_b(y^*, t^*) =$$

$$\frac{K}{m} - \frac{K}{m}e^{-mt^*} + \left[\frac{1-e^{-2m\left(\frac{L-l}{d}\right)}}{e^{-mb} - e^{ma}}\right] e^{-my^*}$$

$$-D\left[\frac{1+e^{-2m\left(\frac{L-l}{d}\right)}}{e^{-mb} - e^{ma}}\right] e^{-my^*} + \left(\frac{1}{2}\right) e^{-mt^*}$$

$$- 2e^{-mt^*} \sum_{n=1+r}^{\infty} (jasin\,(a - t^* + y^*)j$$

$$-jbsin(b + t^* - y^*)j)/((jasin(ja) - jbsin(jb))^2$$

$$+(jacos(ja) + jbcos(jb))^2)$$

$$+2e^{-mt^*} \sum_{n=1+r}^{\infty} (mbcos(b + t^* - y^*)j$$

$$+macos(a - t^* + y^*)j - jbsin(b + t^* - y^*)j$$

$$+jasin(a - t^* + y^*)j)/$$

$$((mbcos(jb) + macos(ja) - jbsin(jb) + jasin(ja))^2$$

$$+(masin(ja) - mbsin(jb) - bjcos(jb) - ajcos(ja))^2)$$

$$-2De^{-mt^*} \sum_{n=1+r}^{\infty} (mbcos(b + t^* - y^*)j$$

$$+macos(a - t^* + y^*)j - jbsin(b+t^* - y^*)j$$

$$+jasin(a - t^* + y^*)j)/$$

$$((mbcos(jb) + macos(ja) - jbsin(jb) + jasin(ja))^2$$

$$+(masin(ja) - mbsin(jb) - bjcos(jb) - ajcos(ja))^2)$$

$$r = 0,2,4 \ldots \quad \text{.....(13)}$$

$$\theta_b(y^*, t^*) = \frac{Q}{m} - \frac{Q}{m}e^{-mt^*} +$$

$$\left[\frac{1 - e^{-2m\left(\frac{L-l}{d}\right)}}{e^{-mb} - e^{ma}}\right] e^{m(k_1 - y^*)} -$$

$$D\left[\frac{1 + e^{-2m\left(\frac{L-l}{d}\right)}}{e^{-mb} - e^{ma}}\right] e^{m(k_1 - y^*)} + De^{m\left(\frac{l}{d} - y^*\right)}$$

$$+e^{m\left(\frac{l}{d}-y^*\right)} - e^{-mt^*} + \left(\frac{1}{2}\right) e^{-mt^*}$$

$$- 2e^{-mt^*} \sum_{n=1+r}^{\infty} (jasin\,(a - k_1 - t^* + y^*)j$$

$$-jbsin(b + k_1 + t^* - y^*)j)/((jasin(ja) - jbsin(jb))^2$$

$$+(jacos(ja) + jbcos(jb))^2)$$

$$+2e^{-mt^*} \sum_{n=1+r}^{\infty} (mbcos\,(b + k_1 + t^* - y^*)j$$

$$+macos(a - k_1 - t^* + y^*)j - jbsin(b+k_1 + t^* - y^*)j$$

$$+jasin(a - k_1 - t^* + y^*)j)/$$

$$((mbcos(jb) + macos(ja) - jbsin(jb) + jasin(ja))^2$$

$$+(masin(ja) - mbsin(jb) - bjcos(jb) - ajcos(ja))^2)$$

$$-2De^{-mt^*} \sum_{n=1+r}^{\infty} (mbcos\,(b + k_1 + t^* - y^*)j$$

$$+macos(a - k_1 - t^* + y^*)j - jbsin(b+k_1 + t^* - y^*)j$$

$$+jasin(a - k_1 - t^* + y^*)j)/$$

$$((mbcos(jb) + macos(ja) - jbsin(jb) + jasin(ja))^2$$

$$+(masin(ja) - mbsin(jb) - bjcos(jb) - ajcos(ja))^2)$$

$r = 0,2,4 \ldots$ .... (14)

Where $D = \frac{2Ha^2Ec(\frac{l}{d})}{Re}$, $j = \frac{\pi nd}{(2L-2l)}$, $a = \frac{2L-l}{d}$, $b = \frac{2L-3l}{d}$ and $k_1 = 2(\frac{l}{d})$.

4 Problem Two

An analytical model of a side heated free convection loop place in a transverse magnetic field will be studied. In this problem, the bottom part of the loop wall is isothermally heated to T_H and the top part isothermally cooled to T_C.

4.1 The Energy and Momentum Equations

The continuity, energy and momentum equations for one dimensional are

$V_0 =$ constant (15)

The energy equation for $-l \le y \le +l$ and $2L - l \le y \ge -2L + l$

$$\rho C_p \left[v_0 \frac{\partial T_b}{\partial y} \right] = \frac{h}{2d}\{T_w - T_b\} + \sigma {v_0}^2 {B_0}^2 \quad ..(16)$$

And for the regions $-2L + l \le y \le -l$ and $l \le y \le 2L - l$

$$\rho C_p \left[v_0 \frac{\partial T_b}{\partial y} \right] = \sigma {v_0}^2 {B_0}^2 \quad ....(17)$$

The momentum equation for the problem under consideration is

$$0 = -\frac{\partial p}{\partial y} + \rho g - \sigma v_0 {B_0}^2 - \frac{\tau}{d} \quad ....(18)$$

T_w is the loop wall temperature in the isothermal regions defined by:

$T_w = T_H$ for $2L - l \le y \ge -2L + l$ ......(19 a)

$T_w = T_C$ for $-l \le y \le l$ .... (19 b)

We can write down the energy equations (16) and (17) in non-dimensional form through using scaling and order of magnitude analysis. This can be done through introducing the following new quantities:

$$\theta_b = \frac{T_b - T_C}{T_H - T_C}, \; y^* = \frac{y}{d}$$

The substituting of these quantities into equations (16) and (17) gives the energy equations in dimensionless form and they are:

$$\frac{\partial \theta_b}{\partial y^*} + m\theta_b = m + \frac{Ha^2Ec}{Re} \quad (20)$$

for $2L - l \le y \ge -2L + l$ and for $-l \le y \le +l$

$$\frac{\partial \theta_b}{\partial y^*} + m\theta_b = \frac{Ha^2Ec}{Re} \quad ....(21)$$

And the dimensionless form of the energy equations for the insulated region, $-2L + l \le y \le -l$, is

$$\frac{\partial \theta_b}{\partial y^*} = \frac{Ha^2Ec}{Re} \quad ....(22)$$

and for $l \le y \le 2L - l$ is

$$\frac{\partial \theta_b}{\partial y^*} = \frac{Ha^2Ec}{Re} \quad ....(23)$$

From which, by using the continuity condition, the boundary conditions that associated with the energy equations for the right and left sides are

$$\theta_b(-l) = \theta_b(-2L + l) + 2Ha^2Ec(\tfrac{L-l}{d})/Re \quad .... (24)$$

$$\theta_b(2L - l) = \theta_b(l) + 2Ha^2Ec(\tfrac{L-l}{d})/Re \quad .... (25)$$

Where m , Re , Ha and Ec are same as in problem one.

4.2 Method of Solution

The governing equations for this problem are solved analytically.

Equations (20) and (21) are linear differential equation of first order and their solutions, respectively, are

$$\theta_b = 1 + Ae^{-\frac{my}{d}} + \frac{2Ha^2EcPr}{Nu} \quad \text{for } 2L - l \le y \ge -2L + l \quad ....(26)$$

$$\theta_b = Be^{-\frac{my}{d}} + \frac{2Ha^2EcPr}{Nu} \quad \text{for } -l \le y \le +l \quad ....(27)$$

Where the dimensionless parameter m is a form of Stanton number given by St= $\frac{h}{2\rho C_p V_0} = \frac{Nu}{2RePr}$. The other parameters in equations (26) and (27) are the Reynolds number based on the induced velocity, $Re = \frac{V_0 d}{\nu}$; the Nusselt

number, $Nu = \frac{hd}{K}$; the Prandtl number, $Pr = \frac{\nu}{\alpha}$; the Eckert number, $Ec = \frac{{V_0}^2}{C_p \triangle T}$; the temperature difference between hot and the cold side walls, $\triangle T = T_H - T_C$; and the Hartmann number, $Ha = B_0 d \sqrt{\frac{\sigma}{\rho \nu}}$. Solution of equations (22) and (23) in the insulated sections give a linearly increasing bulk temperature due to Joulean heating in each segment. Therefore, the bulk temperature in those segments are given in equations (24)and(25). Using equations (24) and (25) one can find the constants A and B in equations, (26) and (27), these constants are

$$A = \frac{[1 - e^{-2\frac{ml}{d}}]}{[e^{m(\frac{2L-3l}{d})} - e^{-m(\frac{2L-l}{d})}]} - \frac{2Ha^2 Ec(\frac{L-l}{d})}{Re}[\frac{1+e^{-2\frac{ml}{d}}}{e^{m(\frac{2L-3l}{d})} - e^{-m(\frac{2L-l}{d})}}] \quad \text{.....(28)}$$

$$B = e^{-m\frac{l}{d}} + Ae^{m(\frac{2L-2l}{d})} + 2e^{-m\frac{l}{d}} \frac{Ha^2 Ec(\frac{L-l}{d})}{Re} \quad \text{.....(29)}$$

The momentum equation (18) which is

$$\frac{\tau}{d} + \sigma {v_0}{B_0}^2 = -\frac{\partial p}{\partial y} + \rho g \quad \text{.....(30)}$$

Since $\rho = \rho_0(1 - \beta(T_b - T_C))$, substitute the value of ρ into equation (30) we get

$$\frac{\tau}{d} + \sigma {v_0}{B_0}^2 = -\frac{\partial p}{\partial y} + \rho_0 g - \rho_0 \beta (T_b - T_C) g \quad \text{.....(31)}$$

and using

$$\theta_b \triangle T = T_b - T_C \quad \text{.....(32)}$$

Substituting from equation (32) into equation (30) we get

$$\frac{\tau}{d} + \sigma {v_0}{B_0}^2 = -\frac{\partial p}{\partial y} + \rho_0 g - \rho_0 g \beta \triangle T \theta_b \quad \text{.....(33)}$$

Integrated equation (33) around the loop we get

$$\int_{-2L}^{2L} \left(\frac{\tau}{d} + \sigma {v_0}{B_0}^2\right) dy = \int_{-2L}^{2L} \left(-\frac{\partial p}{\partial y} + \rho_0 g - \rho 0 g \beta \triangle T \theta b dy\right.$$

$$4\frac{\tau L}{d} + 4\sigma {v_0}{B_0}^2 L = \rho_0 g \beta \triangle T[+\int_{-2L}^{-2L+l} \theta_b dy + \int_{-2L+l}^{-l} \theta_b dy + -l0\theta b dy - 0l\theta b dy - l2L - l\theta b dy$$

$$-\int_{2L-l}^{2L} \theta_b dy] \quad \text{.....(34)}$$

Where the pressure variations in the loop are only due to gravity. The negative and positive signs of the buoyant terms are related to gravity direction which is positive for the upward going flow and negative for the downward going flow. In each integral segment, the respective bulk temperature are used the isothermal region and insulated region. The flow in the channel is assumed fully developed and the solution of Hartmann [5] for MHD plane-Poiseuille flow with a transverse magnetic field is used to correlate the walls shear stress force to the mean flow velocity v_0 by:

$$\tau = \frac{\mu V_0}{d} Ha^2 \frac{\tanh(Ha)}{Ha - \tanh(Ha)} \quad \text{.....(35)}$$

Using the value of τ in equation (35) and evaluating the integral of the buoyancy term using the temperature distribution obtained in equations (26) and (27), reduces equation (34) to the following:

$$\frac{4\mu V_0 Ha^2 \tanh Ha}{d^2(Ha - \tan hHa)} + 4\sigma V_0 {B_0}^2 = \rho_0 g \beta \triangle T[\frac{-A}{m(\frac{L}{d})} e^{m(\frac{2L-l}{d})} + \frac{A}{m(\frac{L}{d})} e^{2m\frac{L}{d}} + \frac{B}{m(\frac{l}{d})} e^{m\frac{l}{d}} + \frac{B}{m(\frac{l}{d})} e^{-m\frac{l}{d}} + \frac{A}{m(\frac{L}{d})} e^{-2m\frac{L}{d}} - \frac{A}{m(\frac{L}{d})} e^{m(\frac{-2L+l}{d})} - 2\frac{B}{m(\frac{l}{d})} \quad \text{.....(36)}$$

Equation (36) gives a correlation between the induced flow velocity v_0 and the other flow and geometric parameters in the system and can then be reduced to the following non-dimensional correlation:

$$Gr = \frac{4ReHa^2[1 + \frac{\tan hHa}{Ha - \tan hHa}]}{\frac{2PrRe\{F\}}{(\frac{L}{d})Nu}} \quad \text{.....(37)}$$

Where Gr is the Grashof number, $Gr = \frac{g\beta \triangle T d^3}{\nu^2}$, the parameter F is defined as

$$F = -A\left(e^{m(\frac{2L-l}{d})} + e^{m(\frac{-2L+l}{d})}\right) + A\left(e^{2m\frac{L}{d}} + e^{-2m\frac{L}{d}}\right) + B\left(e^{m\frac{l}{d}} + e^{-m\frac{l}{d}}\right) - 2B \quad \text{.....(38)}$$

A and B are the dimensionless terms defined in equations (28) and (29).

5 Problem Three

In this problem, we study the unsteady state of problem two. Where the bottom part of the loop wall is isothermally heated to T_H and the top part isothermally cooled to T_C.

5.1 The Continuity and Energy Equations

The continuity equation for one dimensional can be written as:

$$V_0 = \text{constant} \quad \text{.....(39)}$$

The energy equation for $2L - l \leq y \geq -2L + l$ and $-l \leq y \leq +l$

$$\rho C_p \left[\frac{\partial T_b}{\partial t} + \mathrm{v}_0 \frac{\partial T_b}{\partial y}\right] = \frac{h}{2d}\{T_w - T_b\} + \sigma {\mathrm{v}_0}^2 {B_0}^2 \quad \text{.....(40)}$$

And for the regions $-2L + l \leq y \leq -l$ and $+l \leq y \leq 2L - l$

$$\rho C_p \left[\mathrm{v}_0 \frac{\partial T_b}{\partial y}\right] = \sigma {\mathrm{v}_0}^2 {B_0}^2 \quad \text{.....(41)}$$

in the above equations, we assume that the fluid is incompressible, i.e (ρ=constant), where $\frac{J^2}{\sigma} = \sigma {\mathrm{v}_0}^2 {B_0}^2$ defined in problem one, T_b is the bulk temperature, T_w is the loop wall temperature in the isothermal regions defined by:

T_w=T_H for $2L - l \leq y \geq -2L + l$ ..... (42)

T_w=T_C for $-l \leq y \leq +l$ .....(43)

5.2 Non-dimensional Form of Energy Equation

We can write down the energy equation for both regions, the insulated and isothermal, with exception we will add the unsteady term and as follows

$$\frac{\partial \theta_b}{\partial\, t^*} + \frac{\partial \theta_b}{\partial y^*} + m\theta_b = m + \frac{Ha^2 Ec}{Re} \quad \text{for } 2L - l \leq y \geq -2L + l \text{ ..... (44)}$$

$$\frac{\partial \theta_b}{\partial\, t^*} + \frac{\partial \theta_b}{\partial y^*} + m\theta_b = \frac{Ha^2 Ec}{Re} \text{ for } -l \leq y \leq +l \text{ .....(45)}$$

and the dimensionless form of the energy equations for the insulated regions are

$$\frac{\partial \theta_b}{\partial y^*} = \frac{Ha^2 Ec}{Re} \text{ for } -2L + l \leq y \leq -l \text{ ..... (46)}$$

$$\frac{\partial \theta_b}{\partial y^*} = \frac{Ha^2 Ec}{Re} \text{ for } l \leq y \leq 2L - l \text{ ..... (47)}$$

From which, by using the continuity condition, the boundary conditions that associated with the energy equations for the right and left sides are the same as in equations (24) and (25). And the initial condition is given by equation (12).

5.3 Solution of Problem Three

To solve this problem, the Laplace transformation is used on both side of the energy equation (44) and (45).It is found that there solution, respectively is given by

$$\theta_b(y^*, t^*) = \frac{K}{m} - \frac{K}{m} e^{-mt^*} + \left[\frac{1 - e^{-2m\left(\frac{l}{d}\right)}}{e^{ma} - e^{-mb}}\right] e^{m(k_3 - y^*)} - \frac{2Ha^2 Ec\left(\frac{L-l}{d}\right)}{Re}\left[\frac{1 + e^{-2m\left(\frac{l}{d}\right)}}{e^{ma} - e^{-mb}}\right] e^{m(k_3 - y^*)} - \left(\frac{l}{2(L-l)}\right) e^{-mt^*} + e^{-m\left(\frac{l}{d} + y^*\right)} + \left[\frac{1 - e^{-2m\left(\frac{l}{d}\right)}}{e^{ma} - e^{-mb}}\right] e^{-my^*} - \frac{l}{2(L-l)} e^{-mt^*} - D\left[\frac{1 + e^{-2m\left(\frac{l}{d}\right)}}{e^{ma} - e^{-mb}}\right] e^{-my^*} +$$

$$e^{-mt^*} \sum_{n=1}^{\infty} (jasin\big((t^* - y^* - a)j\big) + jbsin\big((t^* - y^* + b)j\big) - macos\big((a - t^* + y^*)j\big) - mbcos((b + t^* - y^*)j))/$$

$$\big(\big(jbsin(jb) - jasin(ja) - mbcos(jb) - macos(ja)\big)^2 + (jbcos(jb) + jacos(ja) + mbsin(jb) - masin(ja))^2\big)$$

$$(-jasin((t^* - k_2 - y^* - a)j) - jbsin\big((t^* - k_2 - y^* + b)j\big) + macos\big((a - t^* + k_2 + y^*)j\big) + mbcos((b + t^* - k_2 - y^*)j))/$$

$$\big(\big(jbsin(jb) - jasin(ja) - mbcos(jb) - macos(ja)\big)^2 + (jbcos(jb) + jacos(ja) + mbsin(jb) - masin(ja))^2\big)$$

$$-e^{-mt^*} \sum_{n=1}^{\infty} (jbsin\,(t^* - y^* + b)j) + jasin\big((t^* - y^* - a)j\big) - jbsin\big((t^* - k_2 - y^* + b)j\big) - jasin((t^* - k_2 - y^* - a)j))/$$

$$\big(\big(jbsin(jb) - jasin(ja)\big)^2 + (jbcos(jb) + jacos(ja)\,)^2\big)$$

$$-De^{-mt^*} \textstyle\sum_{n=1}^{\infty} (jasin\big((t^* - y^* - a)j\big) + jbsin\big((t^* - y^* + b)j\big) - macos\big((a - t^* + y^*)j\big) - mbcos((b + t^* - y^*)j))/((jbsin(jb) - jasin(ja) - mbcos(jb) - macos(ja)\,)^2 + (jbcos(jb) + jacos(ja) + mbsin(jb) - masin(ja))^2\,) +$$

$$(+jasin((t^* - k_2 - y^* - a)j) + jbsin((t^* - k_2 - y^* + b)j) - macos\big((a - t^* + k_2 + y^*)j\big) - mbcos((b + t^* - k_2 - y^*)j))/$$

$$\big(\big(jbsin(jb) - jasin(ja) - mbcos(jb) - macos(ja)\big)^2 + (jbcos(jb) + jacos(ja) + mbsin(jb) - masin(ja))^2\big)$$

$n = 1,2,3, \ldots$ .....(48)

$$+De^{-m\left(\frac{l}{d}+y^*\right)} - e^{-mt^*} -$$
$$e^{-mt^*}\sum_{n=1}^{\infty}(jbsin\,(t^*+k_3-y^*+b)j$$
$$+jasin(t^*+k_3-y^*-a)j - jbsin(t^*+k_3-k_2-y^*+b)j$$
$$-jasin(t^*+k_3-k_2-y^*-a)j)/$$
$$((jbsin(jb)-jasin(ja))^2$$
$$+(jbcos(jb)+jacos(ja))^2)$$
$$+e^{-mt^*}\sum_{n=1}^{\infty}(jasin\left((t^*+k_3-y^*-a)j\right)$$
$$+jbsin\left((t^*+k_3-y^*+b)j\right)$$
$$-macos\left((a-t^*-k_3+y^*)j\right)$$
$$-mbcos((b+t^*+k_3-y^*)j))/$$
$$((jbsin(jb)-jasin(ja)-mbcos(jb)-macos(ja))^2$$
$$+(jbcos(jb)+jacos(ja)+mbsin(jb)-masin(ja))^2)$$
$$+(-jasin((t^*+k_3-k_2-y^*-a)j)$$
$$-jbsin\left((t^*+k_3-k_2-y^*+b)j\right)$$
$$+macos\left((a-t^*-k_3+k_2+y^*)j\right)$$
$$+mbcos((b+t^*+k_3-k_2-y^*)j))/$$
$$((jbsin(jb)-jasin(ja)-mbcos(jb)-macos(ja))^2$$
$$+(jbcos(jb)+jacos(ja)+mbsin(jb)-masin(ja))^2)$$
$$-De^{-mt^*}\sum_{n=1}^{\infty}(jasin\left((t^*+k_3-y^*-a)j\right)$$
$$+jbsin\left((t^*+k_3-y^*+b)j\right)$$
$$-macos\left((a-t^*-k_3+y^*)j\right)$$
$$-mbcos((b+t^*+k_3-y^*)j))/$$
$$((jbsin(jb)-jasin(ja)-mbcos(jb)-macos(ja))^2$$
$$+(jbcos(jb)+jacos(ja)+mbsin(jb)-masin(ja))^2)$$
$$+(+jasin((t^*+k_3-k_2-y^*-a)j)$$
$$+jbsin\left((t^*+k_3-k_2-y^*+b)j\right)$$
$$-macos\left((a-t^*-k_3+k_2+y^*)j\right)$$
$$-mbcos((b+t^*+k_3-k_2-y^*)j))/$$
$$((jbsin(jb)-jasin(ja)-mbcos(jb)-macos(ja))^2$$
$$+(jbcos(jb)+jacos(ja)+mbsin(jb)-masin(ja))^2)$$

$n = 1,2,3, \ldots$ ..... (49)

Where $= \frac{\pi nd}{(2L-2l)}$, $D = \frac{2Ha^2Ec(\frac{L-l}{d})}{Re}$, $k_2 = (\frac{l}{d})$, $k_3 = 2(\frac{L-l}{d})$, $a = \frac{2L-3l}{d}$ and $b = \frac{2L-l}{d}$.

6. Results and Discussion (Problem One)

In this section we will study the effect of the time, Reynolds and Prandtl numbers on the dimensionless bulk temperature distribution, equations (13) and (14), along the loop at $\frac{L}{d} = 20$, $\frac{l}{d} = 2$, $Nu = 1.86$, $Ha = 1$ and $Ec = 0$, as given by [2].

6.1 Effect of Time

To study the effect of time (t^*) on the temperature, we keep Reynolds and Prandtl numbers are fixed, while time is varied from $\pi/6$ to π. We will take Reynolds number is equal 50 and Prandtl number was set into 7, see Figs. (2-6).The following results were observed

1-For the same points, we note that as t^* increases the bulk temperature increases.

2-The bulk temperature varied between -0.015 to 0.02 as t^* increases.

6.2 Effect of Reynolds Number

To study the effect of Reynolds number on the temperature, we have set t^* is equal to $\pi/3$ and Prandtl is equal to 1, while Reynolds is varied from 5 to 150, see Figs. (7-11). The following results were observed

1-For the same points, as Reynolds number increases the bulk temperature decreases.

2-When Reynolds number, $Re \leq 10$, there exist a gradually translate in the bulk temperature.

3-When Reynolds number, $Re > 10$, we note that the transition in the bulk temperature is more rapid from the case of $Re \leq 10$. (increasing in the curvature of the θ_b curve).

6.3 Effect of Prandtl Number

To study the effect of Prandtl number on the temperature, we have set t^* is equal to $\pi/4$ and Reynolds number is equal to 50, while Prandtl number varied from 0.003 to 7, as shown in Figs. (3) and (12-16). The following results were observed

1-For the same points, as Prandtl number increases the bulk temperature decreases.

2-When Prandtl number, $Pr < 0.05$, there exist a sharper translate in the bulk temperature.

3-When Prandtl number, $0.05 < Pr < 1$, there exist a gradually translate in the bulk temperature.

4-When Prandtl number, $Pr \geq 1$, the translation in the bulk temperature becomes faster.

7. Results and Discussion (Problem Two)

In this section, we will study the effect of the Reynolds and Prandtl numbers on the dimensionless bulk temperature distribution, equations (26) and (27), along the loop at $\frac{L}{d} = 20$, $\frac{l}{d} = 2$, $Nu = 1.86$, $Ha = 1$ and $Ec = 0$. Also, we find the effect of Reynolds and Prandtl numbers on the parameter F.

7.1 Effect of Reynolds Number

To study the effect of Reynolds number on the temperature, we keep Prandtl number fixed and is equal to 1, while Reynolds number varied from 10 to 150, see Figs. (17-21). The following results were observed

1-For the same points, as Reynolds number increases the bulk temperature increases.

2-When Reynolds number increases the range of the bulk temperature decreases.

7.2 Effect of Prandtl Number

To study the effect of Prandtl number on the temperature, we keep Reynolds number fixed and is equal to 50, while Prandtl number varied from 0.003 to 7, as shown in Figs. (22-26). The following results were observed.

1-For the same points, as Prandtl number increases the bulk temperature increases.

2-When Prandtl number, $Pr < 1$, the bulk temperature between zero and one.

3-When Prandtl number, $Pr \geq 1$, the bulk temperature exceed the one by small amount.

7.3 Effect of Reynolds and Prandtl Numbers on Parameter *F*

The effect of Reynolds and Prandtl numbers on the parameter F, equation,(37), is analyzed through plotting many cases for the parameter F, as shown in Figs. (27-30). The following results were noted.

1-For all values of Reynolds and Prandtl numbers the parameter F is bounded below and goes to zero.

2-For low to moderate Reynolds number and as Prandtl number increases the range of the parameter F decreases.

8. Results and Discussion (Problem Three)

In this section, we will study the effect of the time, Reynolds and Prandtl numbers on the dimensionless bulk temperature distribution, equations, (48) and (49), along the loop at $\frac{L}{d} = 20$, $\frac{l}{d} = 2$, $Nu = 1.86$, $Ha = 1$ and $Ec = 0$.

8.1 Effect of Time

To study the effect of time (t^*) on the temperature, we keep Reynolds and Prandtl numbers are fixed, while time is varied from $\pi/6$ to π. We have set Reynolds number is equal to 50 and Prandtl number was set into 0.1, as shown in Figs. (31-35). The following results were observed

1-For the same points, we not that as t^* increases the bulk temperature increases.

2-Obviously from the graphs and since the slop of the vertical part from the curve is small then the change of the bulk temperature is small too.

8.2 Effect of Reynolds Number

To study the effect of Reynolds number on the temperature, we have set t^* equal to $\pi/6$ and Prandtl number is equal to 1, while Reynolds number is varied from 10 to 150, see Figs. (36-40). The following results were observed.

1-For the same points, as Reynolds number increases the bulk temperature increases.

2-When Reynolds number increases, there exist a small change in the bulk temperature.

8.3 Effect of Prandtl Number

To study the effect of Prandtl number on the temperature, we have set t^* equal to $\pi/3$ and Reynolds number is equal 50, while Prandtl number varied from 0.003 to 7, as shown in Figs. (41-44). The following results were observed.

1-For the same points, as Prandtl number increases the change of the bulk temperature decreases, and the amount of the change is small, since there exist a small slop in the vertical part.

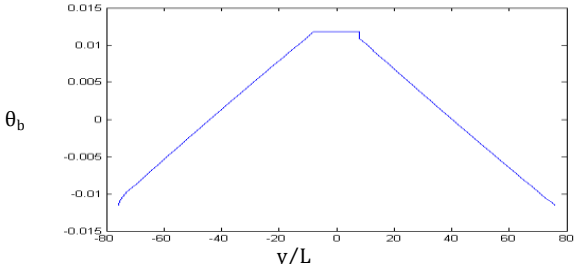

Fig. (2) The dimensionless bulk temperature distribution,θ_b,along. the loop for$\frac{L}{d} = 20, \frac{l}{d} = 2$,Nu=1.86,Re=50,Pr=7,Ha=1,Ec=0 $t^*=\pi/6$.

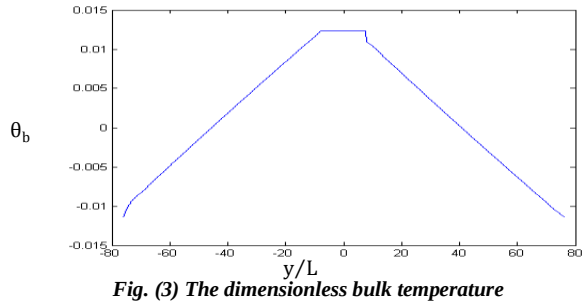

Fig. (3) The dimensionless bulk temperature distribution,θ_b,along the loop for$\frac{L}{d}=20,\frac{l}{d}=2$,Nu=1.86,Re=50,Pr=7,Ha=1,Ec=0 $t^*=\pi/4$.

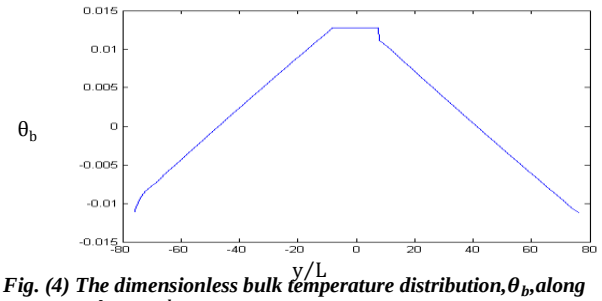

Fig. (4) The dimensionless bulk temperature distribution,θ_b,along the loop for$\frac{L}{d}=20,\frac{l}{d}=2$,Nu=1.86,Re=50,Pr=7,Ha=1,Ec=0&$t^*=\pi/3$.

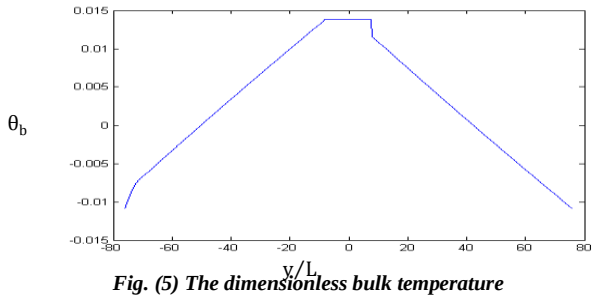

Fig. (5) The dimensionless bulk temperature distribution,θ_b,along the loop for$\frac{L}{d}=20,\frac{l}{d}=2$,Nu=1.86,Re=50,Pr=7,Ha=1,Ec=0 $t^*=\pi/2$.

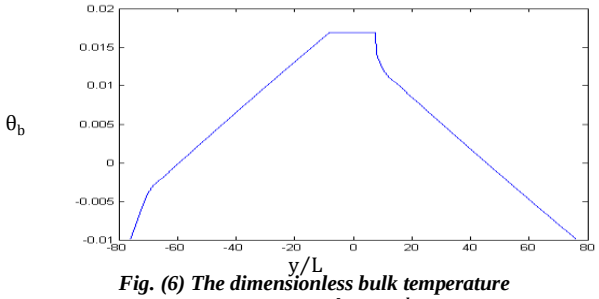

Fig. (6) The dimensionless bulk temperature distribution,θ_b,along the loop for$\frac{L}{d}=20,\frac{l}{d}=2$,Nu=1.86, Re=50,Pr=7,Ha=1,Ec=0 &$t^*=\pi$.

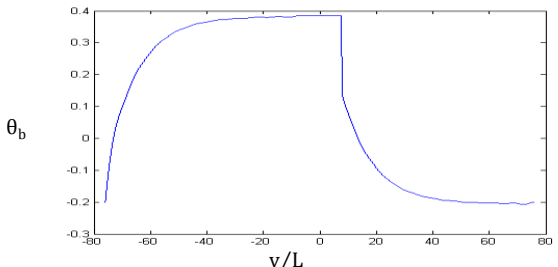

Fig. (7) The dimensionless bulk temperature distribution,θ_b,along the loop for$\frac{L}{d}=20,\frac{l}{d}=2$,Nu=1.86, Re=5,Pr=1,Ha=1,Ec=0, $t^*=\pi/3$.

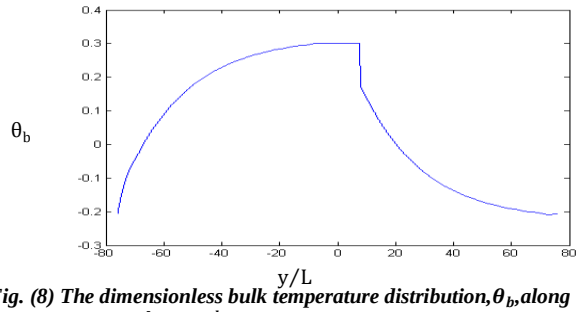

Fig. (8) The dimensionless bulk temperature distribution,θ_b,along the loop for$\frac{L}{d}=20,\frac{l}{d}=2$,Nu=1.86,Re=10,Pr=1,Ha=1, Ec=0, $t^*=\pi/3$.

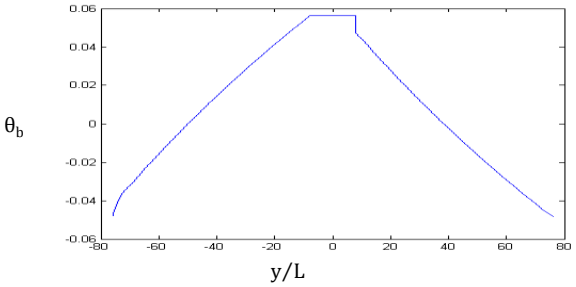

Fig. (9) The dimensionless bulk temperature distribution,θ_b,along the loop for$\frac{L}{d}=20,\frac{l}{d}=2$,Nu=1.86,Re=80,Pr=1,Ha=1,Ec=0, $t^*=\pi/3$

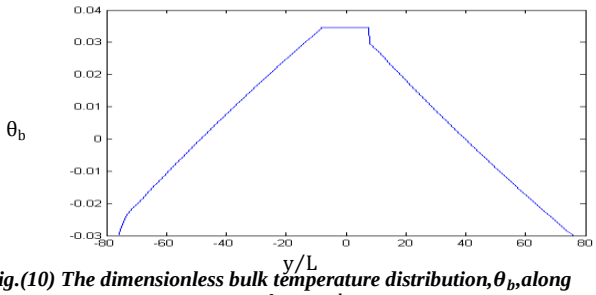

Fig.(10) The dimensionless bulk temperature distribution,θ_b,along the loop for$\frac{L}{d}=20,\frac{l}{d}=2$, Nu=1.86,Re=130,Pr=1,Ha=1,Ec=0&$t^*=\pi/3$.

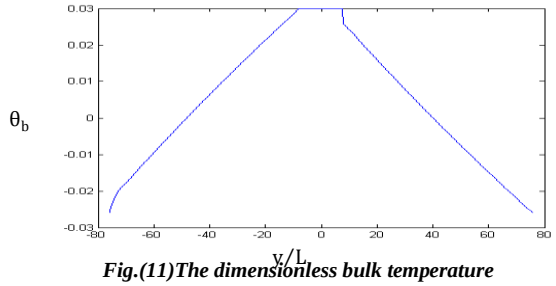

Fig.(11)The dimensionless bulk temperature distribution,θ_b,along the loop for$\frac{L}{d}=20,\frac{l}{d}=2$,Nu=1.86,Re=150,Pr=1,Ha=1,Ec=0, $t^*=\pi/3$.

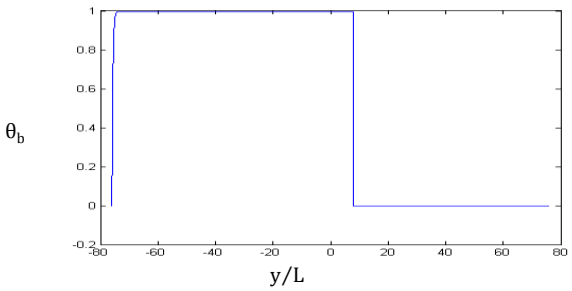

Fig.(12) The dimensionless bulk temperature distribution,θ_b,along theloop for$\frac{L}{d}=20,\frac{l}{d}=$,Nu=1.86,Re=50, Pr=.003,Ha=1,Ec=0, $t^*=\pi/4$.

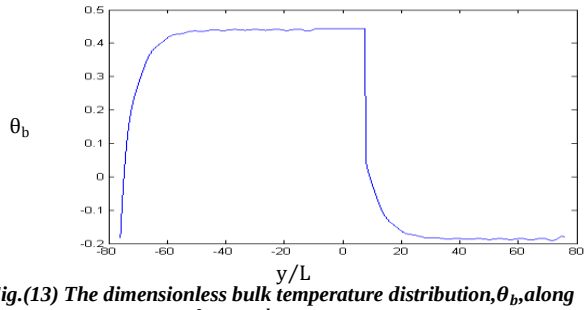

Fig.(13) The dimensionless bulk temperature distribution,θ_b,along the loopfor$\frac{L}{d}=20,\frac{l}{d}=2$,Nu=1.86,Re=50, Pr=.05,Ha=1,Ec=0&$t^*=\pi/4$.

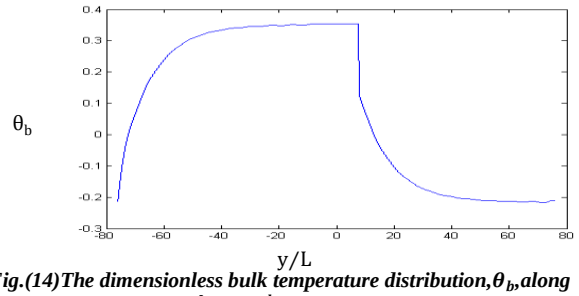

Fig.(14)The dimensionless bulk temperature distribution,θ_b,along the loop for$\frac{L}{d}=20,\frac{l}{d}=2$,Nu=1.86,Re=50, Pr=.1,Ha=1,Ec=0&$t^*=\pi/4$.

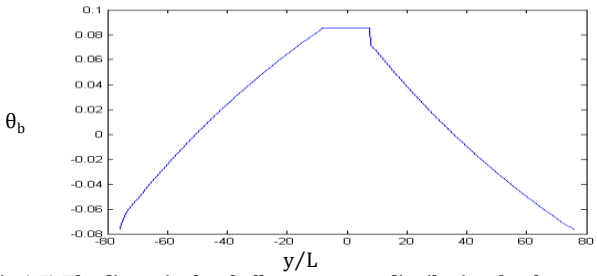

Fig.(15) The dimensionless bulk temperature distribution,θ_b,along the loop for$\frac{L}{d}=20,\frac{l}{d}=2$,Nu=1.86, e=50, Pr=1,Ha=1,Ec=0&$t^*=\pi/4$.

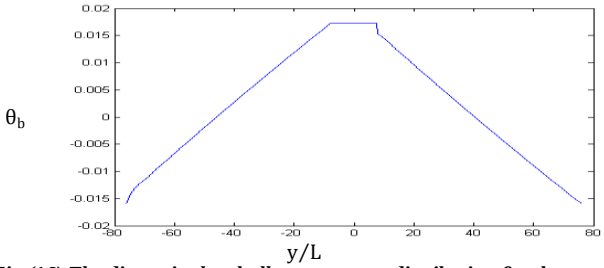

Fig.(16) The dimensionless bulk temperature distribution,θ_b,along the loop for$\frac{L}{d}=20,\frac{l}{d}=2$,Nu=1.86,Re=50, Pr=5,Ha=1,Ec=0, $t^*=\pi/4$.

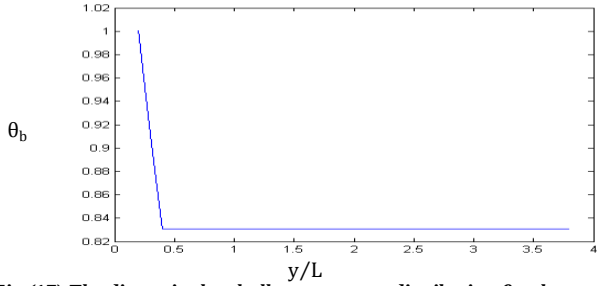

Fig.(17) The dimensionless bulk temperature distribution,θ_b,along the loop for$\frac{L}{d}=20,\frac{l}{d}=2$,Nu=1.86,Re=10, Pr=1,Ha=1&Ec=0.

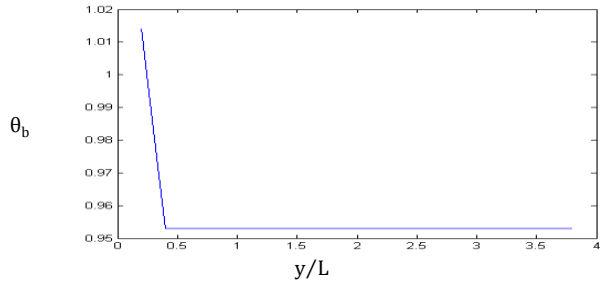

Fig.(18) The dimensionless bulk temperature distribution θ_b,along the loop for$\frac{L}{d}=20,\frac{l}{d}=2$,Nu=1.86, Re=30, Pr=1,Ha=1&Ec=0.

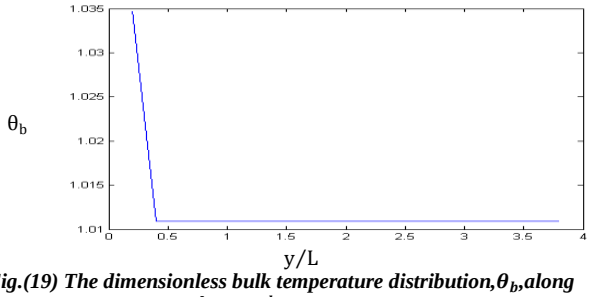

Fig.(19) The dimensionless bulk temperature distribution,θ_b,along the loop for$\frac{L}{d}=20,\frac{l}{d}=2$,Nu=1.86,Re=80, Pr=1,Ha=1&Ec=0.

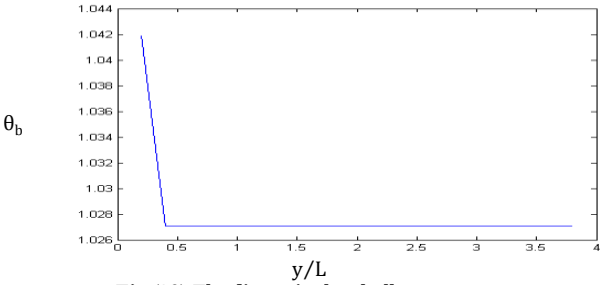

Fig.(20) The dimensionless bulk temperature distribution,θ_b,along the loop for$\frac{L}{d}=20,\frac{l}{d}=2$,Nu=1.86, Re=130,Pr=1,Ha=1&Ec=0.

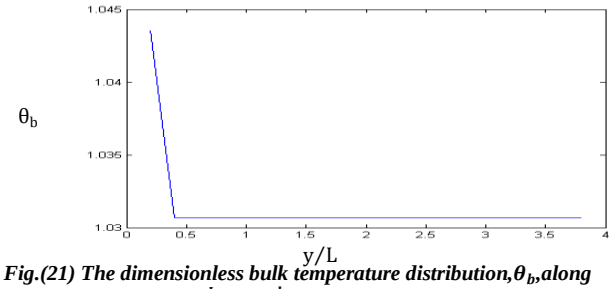

Fig.(21) The dimensionless bulk temperature distribution,θ_b,along the loop for$\frac{L}{d}=20,\frac{l}{d}=2$,Nu=1.86, Re=150, Pr=1,Ha=1&Ec=0.

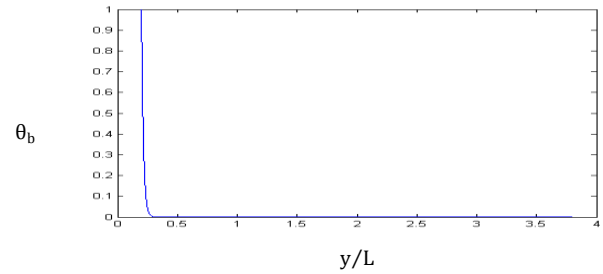

Fig.(22) The dimensionless bulk temperature distribution,θ_b,along the loop for$\frac{L}{d}=20,\frac{l}{d}=2$, Nu=1.86,Re=50,Pr=0.003, Ha=1&Ec=0.

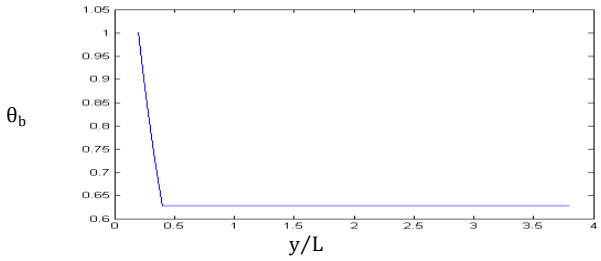

Fig.(23) The dimensionless bulk temperature distribution,θ_b,along the loop for$\frac{L}{d}=20,\frac{l}{d}=2$, Nu=1.86,Re=50 ,Pr=0.08,Ha=1&Ec=0.

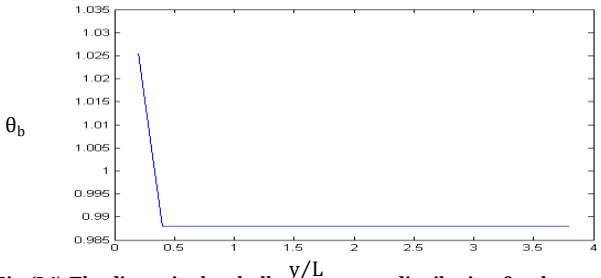

Fig.(24) The dimensionless bulk temperature distribution,θ_b,along the loop for$\frac{L}{d}=20,\frac{l}{d}=2$,Nu=1.86, Re=50, Pr=1,Ha=1&Ec=0.

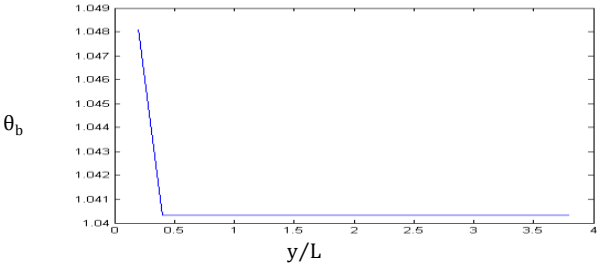

Fig.(25) The dimensionless bulk temperature distribution,θ_b,along the loop for$\frac{L}{d}=20,\frac{l}{d}=2$,Nu=1.86, Re=50, Pr=5,Ha=1&Ec=0.

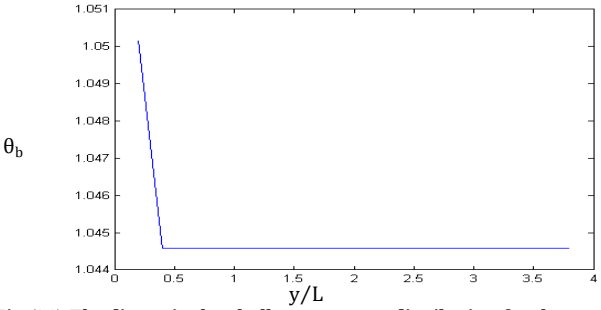

Fig.(26) The dimensionless bulk temperature distribution,θ_b,along the loop for$\frac{L}{d}=20,\frac{l}{d}=2$,Nu=1.86,Re=50, Pr=7,Ha=1&Ec=0.

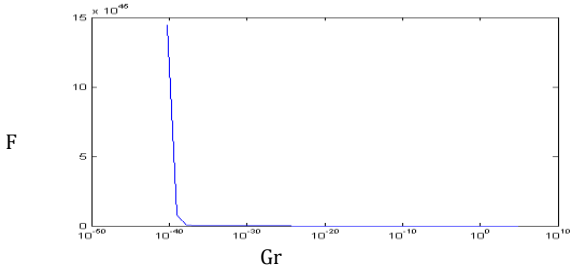

Fig.(27) Aplot of the F parameter as a function of Grashof number for$\frac{L}{d}=20,\frac{l}{d}=2$,Nu=1.86,Ha=5, Ec=0 & Pr=0.003 .

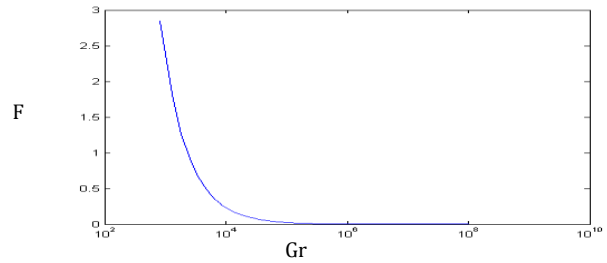

Fig.(28) Aplot of the F parameter as a function of Grashof number for$\frac{L}{d}=20,\frac{l}{d}=2$,Nu=1.86, Ha=5,Ec=0 & Pr=1.

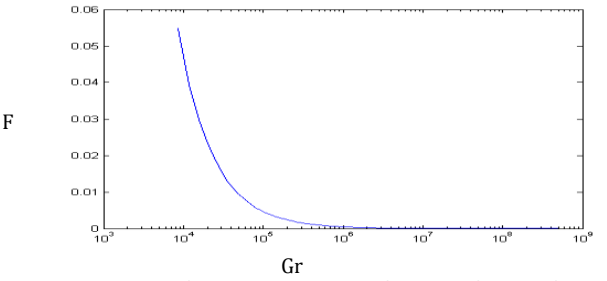

Fig.(29) Aplot of the F parameter as a function of Grashof number for$\frac{L}{d}=20,\frac{l}{d}=2$,Nu=1.86,Ha=5,Ec=0 & Pr=5.

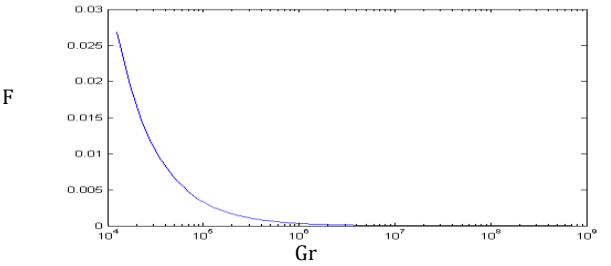

Fig.(30) Aplot of the F parameter as a function of Grashof number for$\frac{L}{d}=20,\frac{l}{d}=2$,Nu=1.86,Ha=5,Ec=0 & Pr=7.

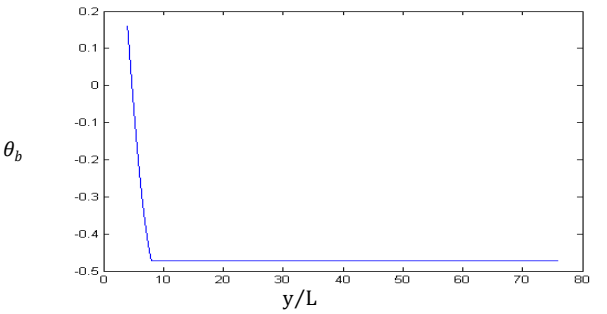

Fig.(31) The dimensionless bulk temperature distribution,θ_b,along the loop for$\frac{L}{d}=20,\frac{l}{d}=2$, Nu=1.86,Re=50, Pr=.1,Ha=1,Ec=0&$t^*=\pi/6$.

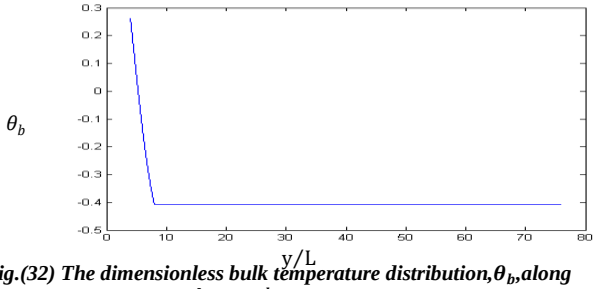

Fig.(32) The dimensionless bulk temperature distribution,θ_b,along the loop for$\frac{L}{d}=20,\frac{l}{d}=2$,Nu=1.86,Re=50, Pr=.1,Ha=1,Ec=0&$t^*=\pi/4$.

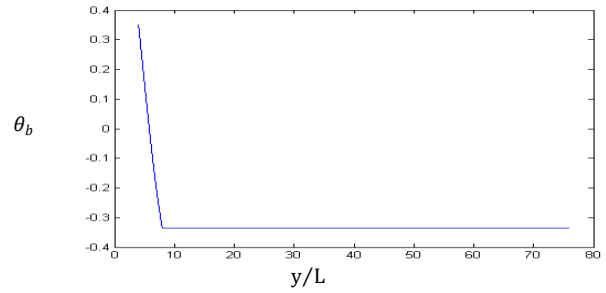

Fig.(33)The dimensionless bulk temperature distribution,θ_b,along the loop for$\frac{L}{d}=20,\frac{l}{d}=2$, Nu=1.86,Re=50,Pr=.1,Ha=1,Ec=0&$t^*=\pi/3$.

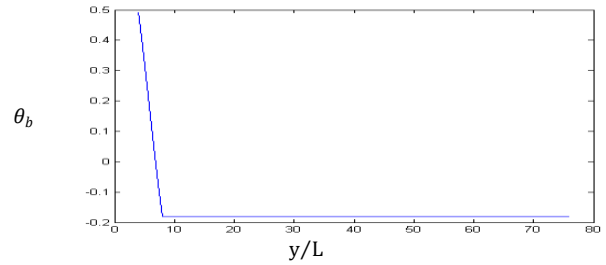

Fig.(34) The dimensionless bulk temperature distribution,θ_b,along the loop for$\frac{L}{d}=20,\frac{l}{d}=2$, Nu=1.86,Re=50, Pr=.1,Ha=1,Ec=0&$t^*=\pi/2$.

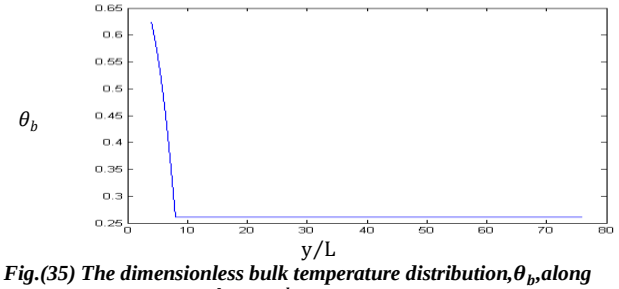

Fig.(35) The dimensionless bulk temperature distribution,θ_b,along the loop for$\frac{L}{d}=20,\frac{l}{d}=2$,Nu=1.86,Re=50, Pr=0.1,Ha=1,Ec=0&$t^*=\pi$.

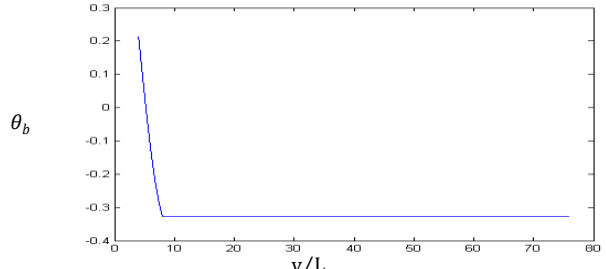

Fig.(36) The dimensionless bulk temperature distribution,θ_b,along the loop for$\frac{L}{d}=20,\frac{l}{d}=2$, Nu=1.86,Re=10,Pr=1,Ha=1,Ec=0&$t^*=\pi/6$.

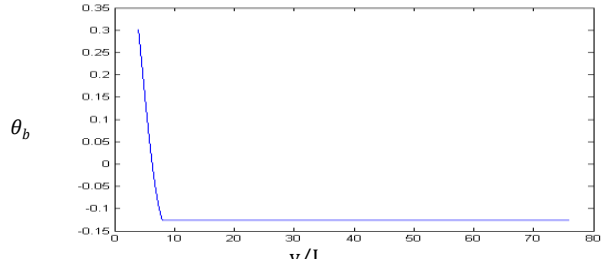

Fig.(37) The dimensionless bulk temperature distribution,θ_b,along the loop for$\frac{L}{d}=20,\frac{l}{d}=2$,Nu=1.86,Re=50, Pr=1,Ha=1,Ec=0&$t^*=\pi/6$.

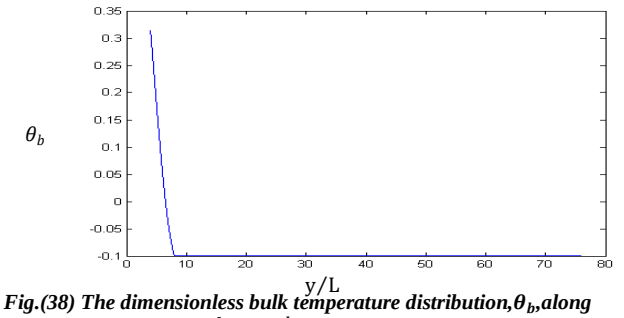

Fig.(38) The dimensionless bulk temperature distribution,θ_b,along the loop for$\frac{L}{d}=20,\frac{l}{d}=2$,Nu=1.86,Re=80, Pr=1,Ha=1,Ec=0&$t^*=\pi/6$.

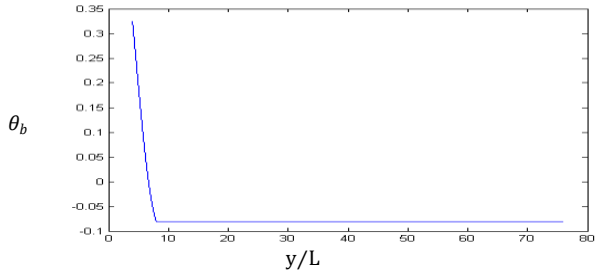

Fig.(39)The dimensionless bulk temperature distribution,θ_b,along the loopfor$\frac{L}{d}=20,\frac{l}{d}=2$,Nu=1.86,Re=130, Pr=1,Ha=1,Ec=0&$t^*=\pi/6$.

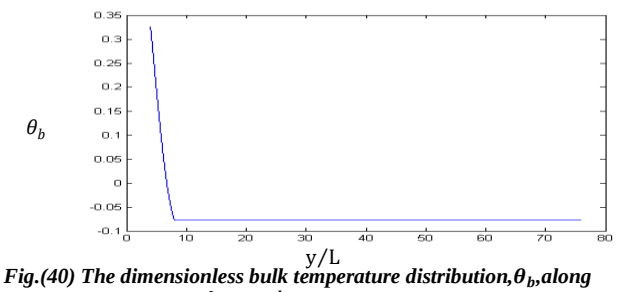

Fig.(40) The dimensionless bulk temperature distribution,θ_b,along the loop for$\frac{L}{d}=20,\frac{l}{d}=2$, Nu=1.86,Re=150, Pr=1,Ha=1,Ec=0&$t^*=\pi/6$.

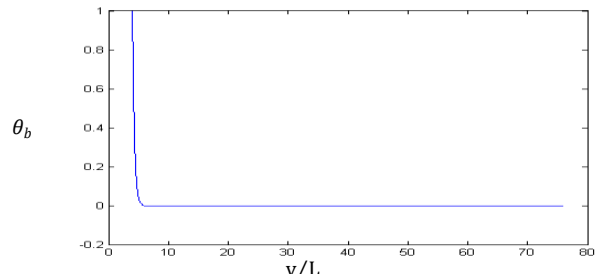

Fig.(41) The dimensionless bulk temperature distribution,θ_b,along the loopfor$\frac{L}{d}=20,\frac{l}{d}=2$, Nu=1.86,Re=50,Pr=.003,Ha=1,Ec=0,$t^*=\pi/3$.

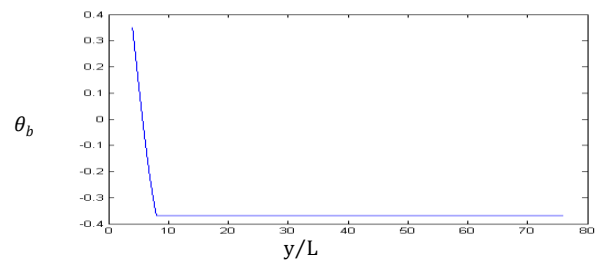

Fig.(42) The dimensionless bulk temperature distribution,θ_b,along the loop for$\frac{L}{d}=20,\frac{l}{d}=2$,Nu=1.86,Re=50, Pr=.08,Ha=1,Ec=0, $t^*=\pi/3$.

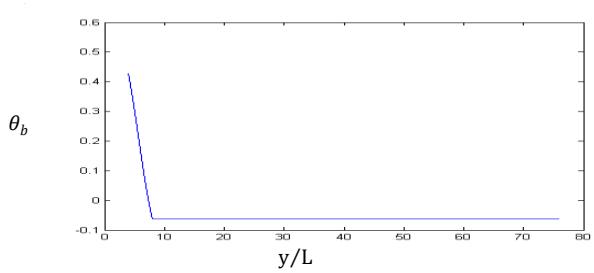

Fig.(43) The dimensionless bulk temperature distribution,θ_b,along the loop for$\frac{L}{d}=20,\frac{l}{d}=2$,Nu=1.86,Re=50, Pr=1,Ha=1,Ec=0&$t^*=\pi/3$.

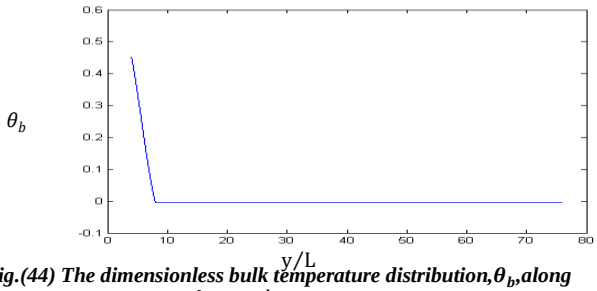

Fig.(44) The dimensionless bulk temperature distribution,θ_b,along the loop for$\frac{L}{d}=20,\frac{l}{d}=2$,Nu=1.86,Re=50, Pr=7,Ha=1,Ec=0&$t^*=\pi/3$.

References

[1] **H. Branover,** Magnetohydrodynamics Flow in Ducts, Wiley, New York. (1978).

[2] **N. Ghaddar,** Analytical Model of a side-Heated Free convection Loop Placed in a Transverse Magnetic Field, Journal of Fluids Engineering, Vol.120, pp. 62-69. (1998).

[3] **K. R. Gramer and S. Pai,** Magnetofluiddynamics for Engineers And Applied Physicists, Mc Graw- Hill, New York. (1973).

[4] **J. E. Hart,** Low Prandtl Number Convection Between Differentially Heated End Walls, International Journal of Heat Mass Transfer,Vol.26, pp. 1069-1074. (1983).

[5] **J. Hartmann,** Hg-Dynamics in a Homogeneous Magnetic Field, Part I, Kg I, Danske Videnskab, Selskab, Mat, Fys. Medd., Vol.15, No.6. (1937).

[6] **K. Sankara Rao,** Introduction to Partial Differential Equations, New Delhi. (1995).

[7] **C. Vives and C. Perry,** Effects of Magnetically Damped Convection During the Controlled Solidification of Metals and Alloys, International Journal of Heat and Mass Transfer, Vol.30, pp.479- 496. (1986).

الخلاصة

تقدم هذهِ الدراسة مميزات هيدروديناميكيه حلقة مغلقه تحتوي على سائل موصل كهربائيا في مجالِ انتقال مغناطيسي في نموذج ذو بعد واحد. درسنا ثلاث مشاكل:في المشكله الاولى درسنا الجريان اللامستقر في حلقه مغلقه وفيها الجانب الأيمن متماثل حرارياً والجانب الأيسر متماثل في البرودهِ، بينما المناطق العليا والسفلى معزوله. في المشكلهِ الثانيه والثالثه درسنا الجريان المستقر واللامستقر في حلقه مغلقه وفيها المنطقه السفلى متماثله حرارياً والمنطقه العليا متماثله في البرودهِ، بينما الجانب الأيمن والأيسر ذو مناطق معزوله.

لقد استخدمنا تحويلات لابلاس لحل المشكلتين الاولى والثالثه، بينما في المشكلهِ الثانيه تم إيجاد الحل لتحليلي.